Journal of Applied Research in Water and Wastewater
E-ISSN: 2476-6283
Journal homepage: https://arww.razi.ac.ir

Adsorptive removal of dyes by utilizing activated carbon-supported copper derived from natural bitumen

Zahra Fadaei[1], Kurosh Rad-Moghadam[*,1], Parvaneh Pakravan[2]

[1]*Department of Chemistry, Faculty of Sciences, University of Guilan, Rasht, Iran.*
[2]*Department of Chemistry, Zanjan Branch, Islamic Azad University, Zanjan, Iran.*

GRAPHICAL ABSTRACT

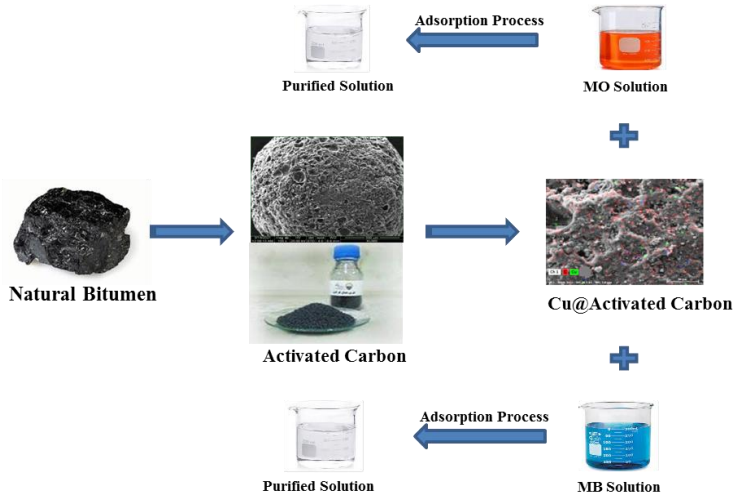

ARTICLE INFO

Article type:
Research Article

Article history:
Received 25 July 2023
Received in revised form 26 September 2023
Accepted 28 September 2023
Available online 30 September 2023

Keywords:
Activated carbon adsorbent
Methyl orange
Methylene blue
Adsorption

ABSTRACT

This study explored the efficacy of a cost-efficient activated carbon (AC) derived from natural bitumen through chemical activation with phosphoric acid. The objective was to evaluate bitumen-based activated carbon (AC) potential as a novel adsorbent by integrating Cu $(NO_3)_2.3H_2O$ onto AC for the removal of harmful dyes from water-based solutions. Assessments of the adsorption capabilities of Cu@AC were conducted using representative samples of cationic and anionic dyes, namely methylene blue (MB) and methyl orange (MO). The incorporation of Cu onto the AC, leading to the formation of Cu@AC, resulted in a significant enhancement of the adsorption capacity of AC. The adsorption capacity of Cu@AC was measured using Brunauer–Emmett–Teller (BET) and iodine number measurements, with the most optimal Cu@AC sample exhibiting a BET surface area of 611 m^2/g. Surface chemical properties were analyzed through FT-IR spectroscopy, while the microstructure of the produced Cu@AC was examined using scanning electron microscopy (SEM) and X-ray diffraction (XRD). The efficiency of the adsorption process was influenced by factors such as pH, initial dye concentration, adsorbent dosage, and contact time. The most effective processing conditions for dye removal were determined as pH 11 for MB and pH 5 for MO, with an initial concentration of 25 mg/L, a 0.5 g/L adsorbent dosage, and a temperature of 333 K for a duration of 90 min. Under these optimized conditions, removal efficiencies exceeded 90% for MO and 80% for MB. The results demonstrated that Cu@AC has the potential to function as a cost-effective alternative to commercially available activated carbons for efficiently eliminating dyes from contaminated water.

1. Introduction

According to Anupam *et al.* (2023), natural bitumen is a mixture of bitumen and natural minerals. It is considered to be an eco-friendly choice and is widely available in different parts of the world. The American Society for Testing and Materials (ASTM) defines bitumen as a black substance with cement-like properties that can be solid, semi-solid, or viscous. This definition includes various materials such as lake bitumen, tars, pitches, and asphaltites. The ASTM also states that asphalt, which is primarily made up of bitumen, can be either naturally occurring or manufactured through industrial processes (Anupam *et al.* 2023). Bitumen is a plentiful natural carbon resource in Canada and is extensively used in the production of hydrocarbon-based substances. In 2017, Canada's crude bitumen production

*Corresponding author Email: radmm@guilan.ac.ir

Cite this article: Z. Fadaei, K. Rad-Moghadam, P. Pakravan, Adsorptive removal of dyes by utilizing Cu supported on activated carbon derived from natural bitumen, *Journal of Applied Research in Water and Wastewater*, 10 (2), 2023, 167-178. doi: https://doi.org/10.22126/arww.2024.9564.1307

reached 2.8 million barrels per day. Unlike regular crude oil, bitumen has higher concentrations of nitrogen, sulfur, and heavy metals. The complexity of bitumen can be reduced *via* fractionation Utilizing various types of solvents, following ASTM standards, allowing the separation of saturates, aromatics, resins, and asphaltenes. Lately, there has been a significant increase in the production of innovative carbon materials, including nanosheets and nanoporous carbon, derived from fossil fuels such as asphaltenes (Mishra *et al.,* 2022).

Natural bitumen displays a range of characteristics including color, hardness, solubility, and volatility, which contribute to its versatility in different applications. Major producers of natural bitumen include Venezuela, Canada, Russia, and countries in the Middle East such as Iran**.** Fig. 1 illustrates the Negin Kabood mine, which provided the source material for this project.

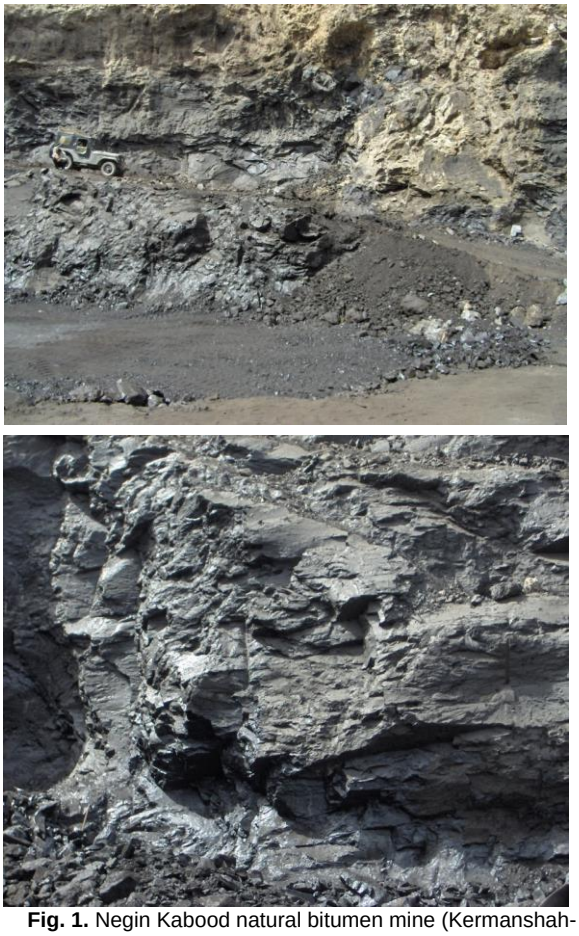

Fig. 1. Negin Kabood natural bitumen mine (Kermanshah-Gilan-e- Gharb).

Activated carbons (ACs) are highly porous materials with multiple surface functionalities, widely used in various applications due to their significant surface area, chemical stability, resistance to heat, and robust mechanical properties. They are derived from both renewable and nonrenewable sources, using either Activation through physical means or treatment with chemicals. Activation by physical means involves converting the precursor into char and then activating it with an oxidizing gas at high temperatures. Chemical treatment, conversely, involves impregnating the precursor with different agents like metal salts and oxidizing agents before thermal activation. The choice of chemical agent significantly influences the structure of the resulting carbon material. By employing various agents, like $FeCl_3$, $ZnCl_2$, KOH, NH_4OH, H_3PO_4, and HCl, for chemical activation, ACs with customizable properties such as high carbon content, adjustable porosity, and tailored surface chemistry can be obtained. This versatility in production techniques allows AC materials to be tailored to meet specific industrial needs and provides a wide range of applications (Ali et al*.,* 2020; Ghasemian Lemraski, Sharafinia and Alimohammadi, 2017) .

AC is extensively utilized across various industries, including pharmaceuticals, chemicals, metallurgy, and petroleum. Its applications are crucial in water treatment, both for purifying water before being distributed and treating industrial effluents. AC is also important in the management of flue gases. Distinct applications of activated carbon in industry encompass the elimination of dyes, the adsorption of heavy metals, and the concentration of precious metals. AC helps to prevent water contamination by removing dyes and ensures compliance with environmental regulations. Additionally, it aids In the process of eliminating contaminants like heavy metals and facilitates the concentration of valuable metals in the mining and metallurgical industry (Cevallos Toledo *et al.,* 2020). These adsorbents can be utilized in dye removal because of their large specific surface area, porosity and surface charge (Xue *et al.,* 2022). The presence of dyes in wastewater has generated apprehension because of their detrimental effects on both human health and the environment. It is vital to address this issue by implementing efficient methods to remove these pollutants from wastewater. Moreover, researchers should focus on finding appropriate techniques for the treatment of such contaminants.

To eliminate dyes from water-based solutions, various methods have been employed, including adsorption, coagulation, flocculation, settling, filtration through membranes, chemical oxidation, electrochemical procedures, catalytic reduction, degradation through photocatalysis, ion swapping, decomposition by microorganisms, membrane-based bioreactors, aerobic and anaerobic biological treatments. (Shahrezaei et al., 2018; Masoudian,; Alsukaibi, 2022). Adsorption has emerged as a straightforward, effective, and cost-efficient technique that utilizes a diverse range of synthetic and natural materials as adsorbents (Rasoulifard and Pakravan, 2015; De Gisi e*t al.,* 2016; Pakravan, 2017; Pakravan, 2018; Abbass *et al*., 2022; Brishti *et al.,* 2023).

Studies have indicated that incorporating copper onto Materials with a significantly large surface area relative to their volume like zeolite, activated carbon fiber, and activated carbon can enhance the distribution of copper oxides and significantly improve catalytic performance due to the presence of numerous active sites. Carbons possessing a significant specific surface area were subjected to alterations involving the inclusion of copper nanoclusters and were evaluated for their potential as materials for hydrogen storage. Copper supported on ZSM-5 catalysts has established a standing as one of the most efficient catalysts for the decomposition of NOx. Utilizing Cu/AC in heterogeneous catalytic ozonation significantly improved the degradation efficiency of nitrobenzene (Hosseini *et al.,* 2015; Abdedayem, Guiza and Ouederni, 2015; Jiang, Zhang and Yan, 2018a; Zhao *et al*., 2020; Quine *et al*., 2022).

The elimination of MO (acidic/anionic dye) and MB (basic/cationic dye) from water is crucial because of their toxicity. MO and MB are selected as representative dyes in their respective categories. Various adsorbents such as activated carbon (Azam *et al.,* 2022), a sugar beet bagasse (SBB) (Ghorbani and Kamari, 2016), alginate bead (Rocher *et al.,* 2008), wastes derived from cellulose material (Annadurai, Juang and Lee, 2002), black tea wastes (Ullah *et al.,* 2022), Zeolitic Imidazolate Frameworks (Lamari, Benotmane and Mostefa, 2022), longan seed-derived activated carbon, treated rice husk (Shafeii Darabi, Bahramifar and Khalilzadeh, 2018), Saccharomyces cerevisiae (Bahramifar, Tavasolli and Younesi, 2015), mesoporous activated carbon (Yu and Luo, 2014) and diaminoethane sporopollenin (Ayar, Gezici and Küçükosmanoğlu, 2007) have been studied for their potential to eliminate dyes, As documented in existing literature (Haque, Jun and Jhung, 2011). The molecular structures of dyes are shown in Scheme 1.

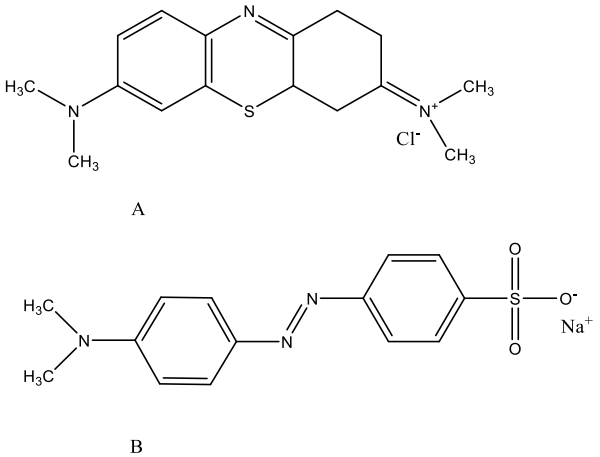

Scheme 1. (a) Molecular structure of methylene blue, and (b) methyl orange.

This study presents the process of creating activated carbon from Persian Prosopis farcta through chemical activation. This study centers on the investigation of removing MO and MB from aqueous solutions using Cu supported activated carbon (Cu@AC). Water contamination resulting from industrial and municipal sewage, along with agricultural activities, is a significant issue in developing countries like Iran. The issue is exacerbated by inadequate factory, industry, and sewage disposal infrastructure, especially in urban regions. The research fine-tuned different operational factors, including initial concentration, pH, time, and temperature, and the findings are now shown.

2. Materials and methods

2.1. Materials and instruments

All the substances employed in this investigation, including H_3PO_4 (99%), HCl (99 %), MO, MB, were of high purity and purchased from Merck (Darmstadt, Germany). All additional chemicals were of analytical quality, and all glass equipment was washed with HNO_3 and rinsed using double-distilled water before use. Natural bitumen was collected from Negin Kabood mine of Iran. The absorption investigations were conducted utilizing Jenway 6305 UV-Vis spectrophotometer. The surface characteristics of the specimens were examined using a scanning electron microscope (SEM) that was outfitted with an energy-dispersive X-ray spectrometer (EDX) (Quantax-Bruker), Fourier-transform infrared spectroscopy (FTIR), and X-ray powder diffraction (XRD) analysis. The characteristic peaks and bands acquired by the IR spectrum of the sample were recorded on a Bomen MB-101 FT-IR spectrometer operating in the range of 4000–400 cm^{-1} using KBr pellets with a resolution of 1 cm^{-1}. The pH of the sample solution was modified by adding HCl or NaOH and then determined using a Jenway model 3510 pH meter.

The XRD patterns were acquired by using a APD2000 GNRX-ray diffractometer (GNR Analytical Instruments Group, Italy) powered with a Cu X-ray source operating at 40 kV voltage and 40 mA current. A Micrometric ASAP 20 surface analyzer was employed to gauge the surface area of the specimens utilizing the Branauer-Emmett-Teller (BET) technique, following the ISO 9277 standard. Before the measurements, all samples were subjected to a 6-hour degassing process at 300°C. The chemical composition was examined through scanning electron microscopy with energy-dispersive X-ray spectroscopy (SEM-EDX) using a Quanta 450 FEG-FEI scanning electron microscope. This microscope was equipped with an EDX Bruker QUANTAX system, and the analysis was conducted at an acceleration voltage of 20 kV. The SEM-EDX analysis involved powder samples affixed to aluminum pin stubs using carbon conductive tapes, and no additional sputtering of another material was applied.

The iodine number is a method utilized to assess the adsorption capacity of activated carbons. It serves as an indicator of the carbon's porosity and is described as the quantity of iodine that can be adsorbed per gram of the carbonaceous specimen at milligram level. By employing the sodium thiosulfate volumetric method, the iodine adsorption is determined. This measurement reflects the level of activity, with a higher number indicating a higher level of activation, typically reported in mg/g and usually falls within the range of 500 to 1200 mg/g. Moreover, the iodine number provides a valuable approximation of the surface area and the presence of micropores in active carbons with a reasonable level of accuracy. It specifically measures the micropore content of the activated carbon, covering a range of 0 to 20 Å (or up to 2 nanometers), through adsorption of iodine from a solution. Additionally, it can be considered a surface area of carbon between 900 and 1100 m^2/g (Saka, 2012). Alongside the iodine number, other parameters such as ball-pan hardness (ASTM 3802) and specific surface area, ascertained through the BET technique, are often used for assessing the properties of activated carbons.

2.2. Preparation of activated carbon

Natural bitumen powder with a particle size of 250 microns was used for production of activated carbon. During various experiments, carbon samples with impregnation ratio of 0.4-1.4 were prepared. In this aim, phosphoric acid with concentrations of 30, 50 and 70 percent by weight and different weight ratio of natural bitumen were agitated at ambient temperature for 30 min until the raw material is completely impregnated with acid and then extruded. The resulting dough is made into granules with 8*20 mesh (1-3 mm). After this stage, 800 grams of the produced granules were loaded into a fixed bed furnace equipped with a temperature controller. The maximum temperature provided by this oven was 1200 °C. The acquired substance was subjected to pyrolysis in a stainless steel reactor, heating it gradually at a rate of 7 degrees Celsius per minute until it reached 600 ºC, where it was held for approximately 2 hr under the protection of a nitrogen gas flow. In the final stage, the activated carbon was further heated in an oven at 110 ºC for 24 hr before it was ready for use. (Danmaliki and Saleh, 2017).

2.3. Incorporation of metals

After the activated carbon had been prepared, it was incorporated with the metals by the following technique. The as-prepared activated carbon (7 g) was dispersed in a mixture of ethanol and water. In another vessel, copper (II) nitrate trihydrate $Cu(NO_3)_2.3H_2O$ (1.03 g) was dissolved in deionized water. The solution was added drop wise to the activated carbon suspension and stirred. The mixture was heated under reflux at 80 ºC overnight. The product was filtered, dried in an oven at 80 °C, and thence maintained under a nitrogen flow for 2 h at 160 ºC.

2.4. Adsorption tests

Two distinctive organic contaminants, specifically MB (a cationic dye) and MO (an anionic dye), were chosen as the focus of this investigation. Varying concentrations (25–65 mg/L) of MB and MO dyes were prepared by dissolving pure dyes in double-distilled water. All batch adsorption experiments were carried out with stirring at 150 rpm and at a temperature of 25 ± 1 ºC. Typically, 0.5 g of AC was introduced into a 1000 mL beaker containing a 500 mL dye solution at the desired initial concentration, and the mixture was vigorously stirred at 150 rpm. The initial pH values of the dye solutions were adjusted to pH 5 using appropriate amounts of 0.1 M HCl or 0.1 M NaOH solutions for both MB and MO solutions. After a specific duration, 5 mL of the mixture was extracted, and the solid within the liquid was isolated by subjecting it to centrifugation at 5000 rpm for 20 minutes. The dye content in the remaining liquid was then quantified using UV-Vis spectroscopy, measuring wavelengths of 665 nm and 468 nm for MB and MO, respectively. The percentage of dye removal, (DR %) at time t, was calculated using the equation provided below (Munyegaju *et al*., 2022):

$$\text{Dye removal } (\text{DR }\%) = \frac{C_0 - C_t}{C_0} \times 100 \quad (1)$$

here, C_0 (mg/L) and C_t (mg/L) represent the dye concentrations at the beginning and at a specific time (minutes) elapsed during the adsorption experiment. The primary influencing factors were examined and summarized in Table 1. The concentration of the remaining dyes was determined through a spectrophotometric method, and the percentages of dyes removal efficiency were calculated.

To investigate the reusability of Cu@AC under the optimal conditions determined for MO and MB adsorption on Cu@AC, 20 mL of MO or MB solution (25 ppm concentration) was introduced to 0.5 g of the adsorbent at pH 5 and a temperature of 333K. Following a 90-minute stirring period, the mixture was filtered, and the adsorbent was isolated to examine it's desorption and regeneration. The desorption process was executed through washing 0.01 g of a dye-loaded adsorbent with 2.0 mL of EtOH, pure acetic acid, HCl (0.1 mol/L) and NaOH (0.1 mol/L) solutions. Cu@AC was collected from the solution by filtration. The dye concentration in the desorbed solution was measured by spectrophotometry.

Table 1. Investigation of various factors on the removal of dyes.

Factors	Range of changes
pH	5-11
Adsorbent dose	0.1 to 0.5 g/L
Temperature	298, 313 and 333 K
Initial concentration of dyes	20-65 mg/L
Contact time	10-90 min
Different reagents and reusability	EtOH, acetic acid, HCl, and NaOH

3. Results and discussion

Chemical and physical reactivation methods were assessed through various acid-washing techniques and thermal treatments in the range of 650 to 950 ºC, respectively. The utilization of H_3PO_4 for activation is becoming more popular because it can introduce carbon-oxygen surface functional groups through grafting. (Ali *et al.,* 2020). Based on existing literature, FT-IR and SEM analysis suggested that the adsorption of MB by AC can be classified as physical adsorption,

which does not alter the structural properties of AC (Wang, Ma and Sun, 2022).

3.1. Characterization
3.1.1. Spectroscopic analysis

FT-IR studies provide crucial insights into identifying the significant functional groups located on surface of the materials that have the ability to adsorb organic contaminants. The FT-IR spectra of AC and Cu@AC are shown in Fig. 2. Both spectra exhibit comparable shapes in the vibration band features of materials composed of carbon, and the highly intense bands found at 3427 cm^{-1} can be attributed to O–H groups caused by moisture content (Elango *et al.,* 2017). The band observed at approximately 2920 cm^{-1} aligns with the C–H stretching vibrations of aliphatic groups. Meanwhile, the bands at around 1500 and 1750 cm^{-1} can be ascribed to the axial deformation of C=O, such as highly conjugated C=O stretching and C=O stretching in alkyl carboxylate groups, respectively. The bands observed at 1049 and 1080 cm^{-1} correspond to C–O stretching of alcohol and ether groups in the structure of Ac. The significant shifts observed for these bands in the FT-IR spectrum of Cu@AC implies that Cu ions have formed strong complexes with the alcoholic and etheric groups of Ac in this composite. (Shu *et al*., 2017). From a comparison between FT-IR spectra of Cu@AC and AC, it is evident that the former exhibits fewer functional groups with reduced intensities. This reduction suggests that many oxygen-containing functional groups on the carbon surface were significantly decreased during the activation process. Fig. 2 displays an additional band at 547 cm^{-1} that is associated to Cu–O vibration, thus indicating the successful incorporation of Cu particles into AC (Sharma *et al*., 2021).

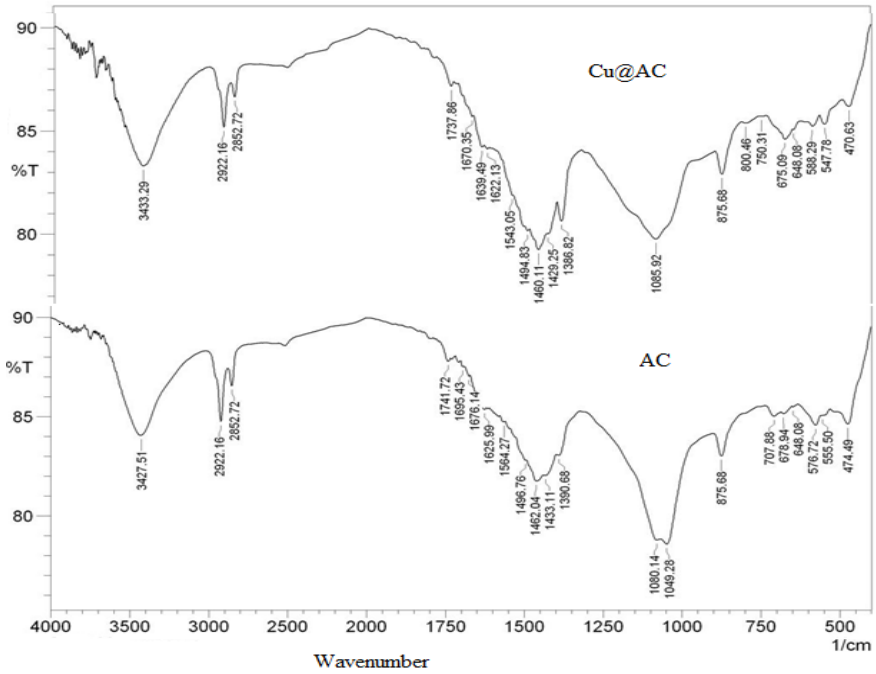

Fig. 2. FT-IR spectra of Cu@AC and AC.

3.1.2. SEM analysis and EDX elemental analysis

SEM-EDX analysis is necessary to determine the morphology and the elements present on surface of AC and Cu@AC. Scanning electron microscopy (SEM) shed light on assessing the surface morphology and texture of AC before and after copper loading.

Clearly, there is a substantial distinction to be made between the surface morphology of AC and Cu@AC. Fig. 3 and Fig. 4 shows the SEM images of AC and Cu@AC. As shown in Fig. 3, pores are abundant around the smooth surface of AC, making it suitable for loading of copper ions onto its surface. Fig. 4 indicates the surface structure of Cu@AC that the even distribution of green copper spheres on the AC surface causes a modification in its surface properties, ultimately leading to enhanced adsorption capacity. From the micrographs, it is evident that the outer surface of AC exhibits cracks, crevices, and some grains in various sizes in large holes. The SEM images obtained from AC post-production through carbonization at 600 °C provide evidence that its porous structure resulted from the release of volatile organic components, leaving behind a ruptured surface with a limited number of pores (Saka, 2012). Studies have indicated that a substantial specific surface area provides an abundance of active sites, and a significant quantity of micropores facilitates the rapid adsorption and reaction of reactants and products within the channels, thereby enhancing the reaction rate (Cui *et al.,* 2020). In this research, Cu@AC exhibits an irregular and a well-developed porous structure with a high amount of defective edges, affording it a relatively high surface area (Fig. 4). After activation, the external surface of AC acquires cracks, crevices, and some grains in various sizes in large holes. During high-temperature activation, the H_3PO_4 content of AC loses water to give P_2O_5. Owing to sublimation, P_2O_5 escapes from the surface of AC, leading to the formation of small pores (Hung *et al.,* 2022).

The elemental composition of the tested samples is evident from the EDX microanalysis presented in Fig. 5 that is in strong accordance with XRD and SEM analysis. All the samples contain carbon, copper and oxygen associated with small amounts of nickel, manganese and calcium which are the natural impurities of the raw bitumene.

In addition to showing the surface morphology, SEM-EDX can be used to determine the elements present on a material surface. Based on Fig. 5, the surface of AC contains the elements of carbon, oxygen, calcium, sulfur and magnesium. According to the EDX spectrum, AC is mainly composed of carbon (~52.91%) and the alkali, alkaline, and sulfur were counted as the minor elements.

In comparison, Cu@AC contains the elements of carbon (C), copper (Cu), nickel (Ni), and gadolinium (Gd). Additionally, EDX analyses of both AC and Cu@AC revealed that AC consists mostly of approximately 52% carbon and 16% oxygen, while the Cu@AC consists of about 27% carbon and 3.82% copper, with small traces of other elements. These spectra indicate that carbon and oxygen are the dominant elements in AC. It is worthy to note that the EDX probe has its limitations and can only identify elements with a content exceeding approximately 0.5%. Consequently, the hydrogen content could not be ascertained using this method (Ngueabouo *et al.,* 2022). Nonetheless, the substantial carbon content indicates the potential suitability of these materials as support agents for pollutant adsorption processes.

It is notable that raw activated carbon contains heavy metals including copper due to the fact that its origin is natural bitumen, and after being modified with copper metal, the percentage of copper has increased, which can be seen in its EDX analysis.

3.1.3. XRD and BET analysis

XRD analysis is a valuable analytical tool for characterizing the crystalline phases in different materials. Each element exhibits a unique diffraction pattern when subjected to X-ray radiation.

XRD patterns were presented for both activated carbon (AC) and metal-loaded AC, as illustrated in Fig. 6. For all samples, diffraction peaks were consistently observed at 2θ values of approximately 26° (002) and 43° (101), indicating the presence of amorphous carbon. In Fig. 6a, The C peaks were assigned according to the pattern JCPDS:04-019-9068 and 04-007-2136 (Trung *et al.,* 2022). In the case of Cu@AC, as shown in Fig. 6b, the XRD pattern for Cu@AC displayed a diffraction peak from the CuO phase at 38.74° (111), JCPDS No. 89-5895, indicating the successful introduction of CuO into the AC. Additionally, a distinct diffraction peak at 2θ = 43.3° was attributed to metallic copper (Cu°) with the (111) plane, referencing JCPDS No. 04-0836. The formation of Cu° resulted from the reduction of CuO by the carbon carrier at high temperatures *(*Jiang *et al.,* 2018b).

The thermal reduction of oxidized samples led to the disappearance of diffraction peaks associated with $Cu(OH)_2$ and the emergence of peaks characteristic of Cu° and CuO phases, signifying the complete transformation of $Cu(OH)_2$ through thermal reduction in a nitrogen atmosphere. This transformation is attributed to processes involving the dehydrating and deoxidizing of the source sample, in agreement with previous research. The presence of Cu° in the prepared sample was further confirmed by the detection of a diffraction peak at 43° (Cui *et al.,* 2020).

Consequently, XRD analysis of Cu@AC (Fig. 6b) revealed a predominantly amorphous structure with a noticeable hump in the 20–30° range, indicative of a significant degree of disorder commonly observed in carbonaceous materials. These results align with earlier investigations on the production of AC from agricultural residues (Vunain, Kenneth and Biswick, 2017). Characterization of Cu@AC was continued by performing the detailed analyses such as determination of its iodine number, ball-pan hardness, and specific surface area, following the standard procedures whose results are presented in Table 2. The most important factor to define a good AC is its hardness. The mechanical property of Cu@AC was evaluated through ball-pan hardness to be the value of 97%. This table shows the BET surface area of the sample obtained from its N_2 adsorption/desorption isotherms. As anticipated, the treated sample displayed a notably high BET surface area of 611 m^2/g for Cu@AC, which can be ascribed to the combined impact of chemical oxidation and high-temperature treatment. This suggests that H_3PO_4-activation not only influenced the surface area of Cu@AC but also stimulated the formation of additional pores during the physical activation process. This might serve as a promising sign of utilizing H_3PO_4 as an activating agent to enhance porosity development. The study showed that Cu@AC exhibited improved carbon characteristics, boasting a substantial specific surface area of 611m^2/g.

Table 2. Analysis of ball-pan hardness (%), iodine number (mg I_2/g) and BET (specific surface area (m^2/g)) of modified activated carbon Cu@AC.

Tests	Cu @AC	Test method
Ball pan hardness (Mass %)	97.0	ASTM D3802
Iodine number (mg I_2/g)	707	ASTM D4607
BET, surface area (m^2/g)	611	ISO 9277

In addition, subjecting the chemically activated samples to physical treatment led to a subsequent rise in pore volume as volatiles were released from within the pores. Moreover, increasing the temperature resulted in a greater extent of microporosity, as carbon burned within the ash structure. The elevated surface porosity significantly improved the sorption properties of the activated AC samples (Ali *et al.,* 2020). The iodine number indicates the quantity of iodine that activated carbon can adsorb per gram (measured 707 mg I_2/g). This characteristic serves as a measure of the adsorption capacity or power of the activated carbon.

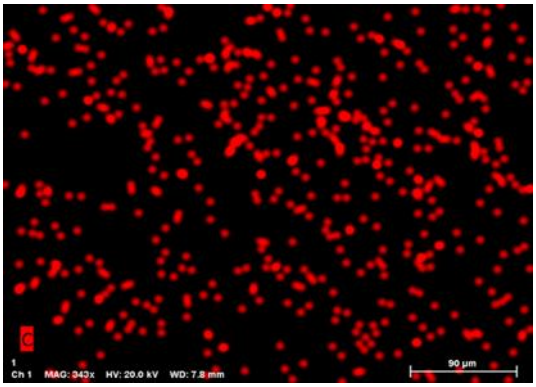

(a)

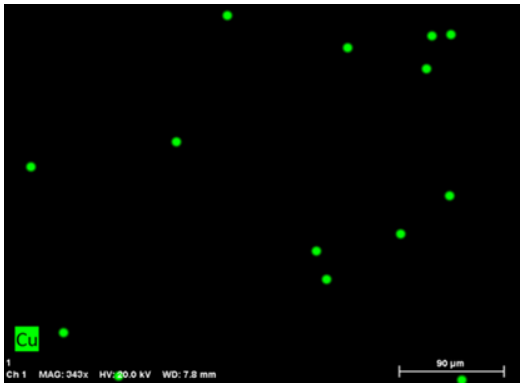

(b)

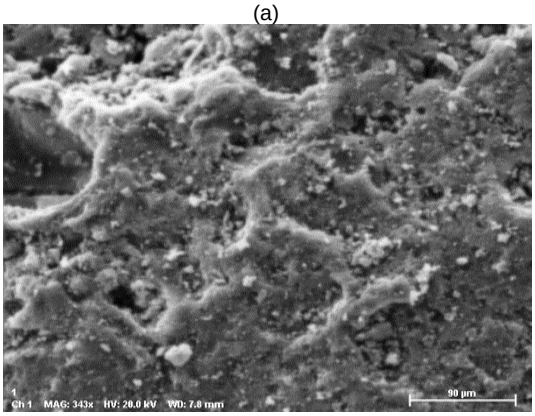

(c)

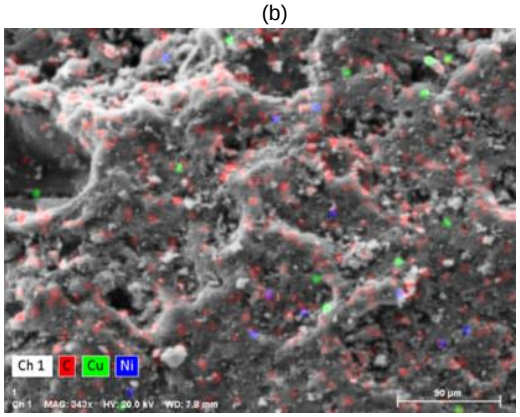

(d)

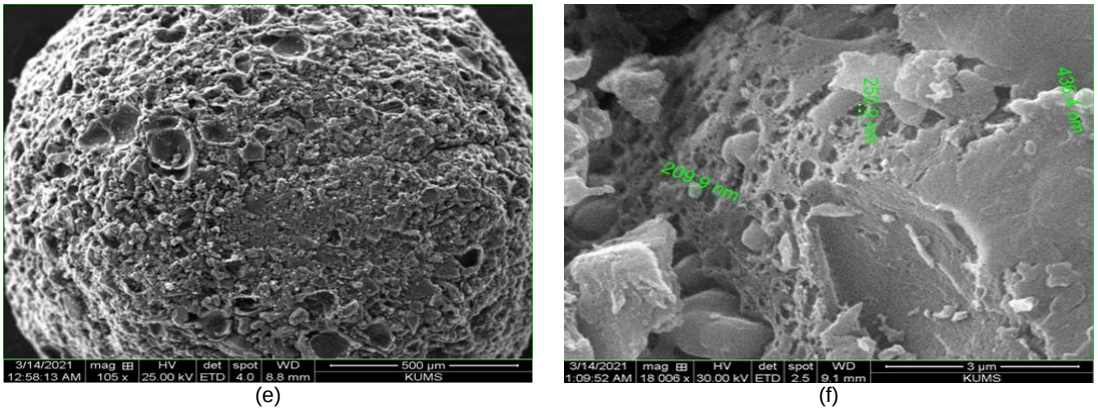

(e) (f)

Fig. 3. SEM image of AC (a) distribution of carbon, (b) distribution of Cu, (c) surface of AC, (d) distribution of C and Cu, (e) granule shape of AC, and (f) pore size of AC.

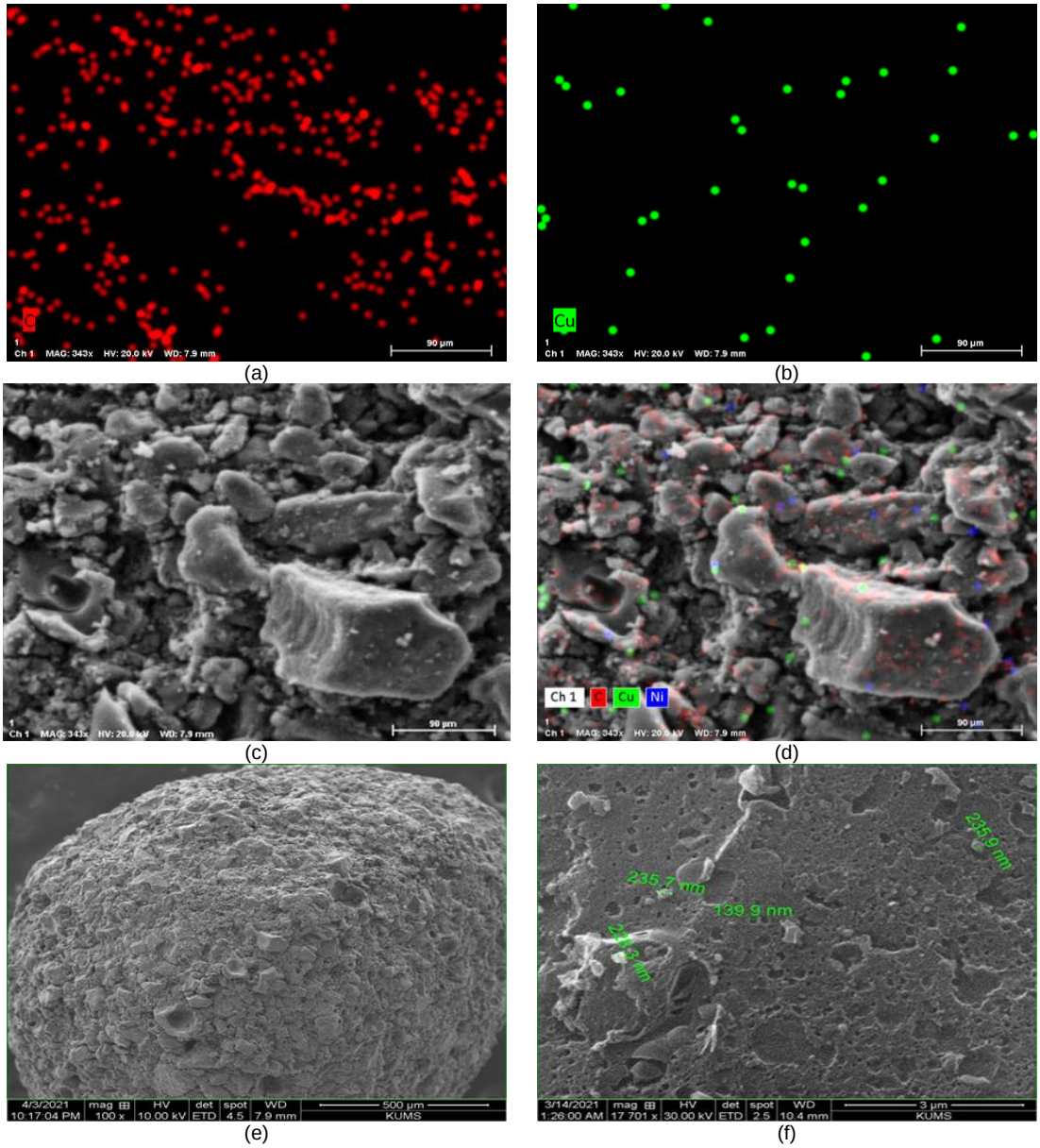

(a) (b)

(c) (d)

(e) (f)

Fig. 4 . SEM image of Cu@AC (a) distribution of carbon, (b) distribution of Cu, (c) surface of AC, (d) distribution of C, Cu, (e) granule shape of Cu@AC, and (f) pore size of Cu@AC.

3.2. Adsorption of Azo Dyes onto Activated Carbon

3.2.1. Effect of pH

The pH of the solution is a significant factor in controlling the dye adsorption process by influencing , the charge of the adsorbent, the structure of the dye molecule, the ionization state of dyes surface, the dissociation of functional groups on the active sites of the adsorbent, and the adsorption capability (Lamari, Benotmane and Mostefa, 2022). Fig. 7 shows the effect of pH on the adsorption of MB and MO onto the Cu@AC at 50 mg/L initial concentration of the dyes and 0.5 g/L of adsorbent. During the adsorption process, when the pH is low, the adsorbent surface becomes positively charged, promoting the adsorption of anionic contaminants. However, since MB is a cationic dye, positive charges residing on the feasible adsorption positions compete with the dye molecules, leading to lower dye adsorption. Conversely, at higher pH levels, the negatively charged surface

facilitates the adsorption of cationic contaminants (Khodaie *et al.,* 2013). Based on the test results, MO dye shows a higher absorption efficiency in acidic pH conditions, while MB dye exhibits a higher absorption efficiency in alkaline pH conditions.

The impact of pH on the adsorption of MB and MO onto the Cu@AC was studied in the range of 5–11 and the findings were demonstrated in Fig. 7. One of the critical factors that influence the adsorption of organic dye ions is the concentration of H^+ or OH^- ions, which leads to the protonation or deprotonation of the functional groups on the adsorbent. The highest adsorption capacities for MB and MO were achieved at pH levels of 11 and 5, respectively, when using an adsorbent dosage of 0.5 g for Cu@AC. At lower pH values, the adsorbent surface becomes positively charged, leading to the attraction of the anionic dye MO through electrostatic forces.

Conversely, at higher pH values, effective adsorption of cationic MB occurs because of the strong electrostatic forces between the positively charged cationic MB dye and the overall negatively charged adsorbent surface in the solution. When the solution pH is above 3.46, which corresponds to the pKa of MO, the anionic MO ions, owing to their sulfonate groups (SO_3^-), are likely drawn towards the positively charged Cu atoms on the adsorbent surface. This condition results in the highest removal efficiency, reaching 100%.

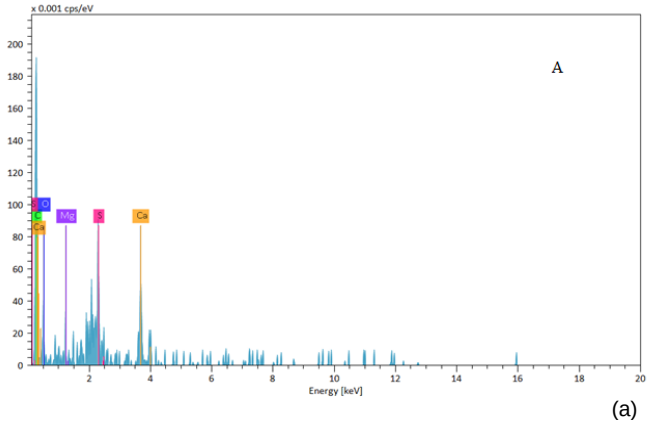

(a)

Element	At. No.	Line S.	Netto	Mass (%)	Atom (%)
Carbon	6	K-Serie	80	52.91	76.89
Oxygen	8	K-Serie	14	16.77	18.29
Calcium	20	K-Serie	47	7.33	3.19
Sulfur	16	K-Serie	37	2.30	1.25
Magnesium	12	K-Serie	8	0.52	0.37
			Sum	79.83	100.00

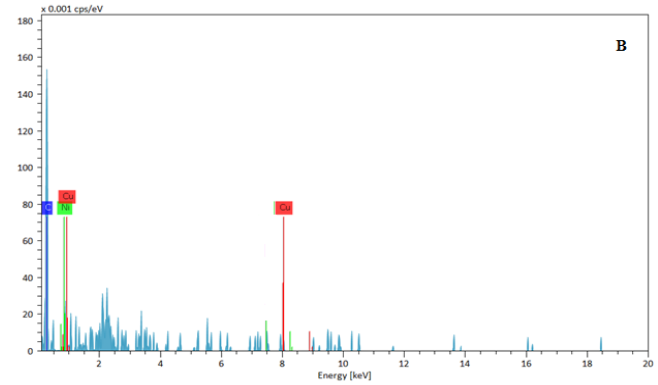

(b)

Element	At. No.	Line S.	Netto	Mass (%)	Atom (%)
Carbon	6	K-Serie	53	27.57	97.03
Copper	29	K-Serie	7	3.82	2.54
Nickel	28	K-Serie	1	0.53	0.38
Gadolinium	64	L-Serie	0	0.18	0.05
			Sum	32.1	100.0

Fig. 5. (a) EDX spectra of AC, and (b) Cu@AC.

On the contrary, MB dye is classified in the group of cationic dyes, due to the partial positive charge of the dye molecule. Hence, its interaction with the cationic adsorbent would increase in alkaline pH domains. As was expected, the removal of MB is more favorable at higher pH values because, as a cationic dye, it tends to be attracted to the adsorbent surface, which becomes negatively charged at these pH levels. Conversely, the maximum adsorption of the anionic MO dye occurs at pH 3 (Kamdod and Kumar, 2022). At lower pH levels, the adsorbent surface acquires a positive charge, which leads to the attraction of the anionic MO dye due to electrostatic forces. Conversely, at higher pH levels, the adsorbent effectively captures the cationic MB dye because of the presence of robust electrostatic attractions arises from the positively charged cationic MB and the overall negatively charged surface of the adsorbent.

3.2.2. Effect of the adsorbent dosage

This effect was studied using different doses of Cu@AC from 0.1 to 0.5 g that was shown in Fig. 8. Results show that the percentage of adsorption is increased by increasing the dose of Cu@AC. It is evident that with an increase in the adsorbent quantity, the number of sorption sites available for interactions between the adsorbent and dye also rises. This leads to an increased percentage of dye removal from the solution. The study revealed that the percentage of dye removal (adsorption capacity) increased linearly with the dosage of the adsorbent. Value of 100 % and 95 % achieved for MO and MB removal, respectively, indicate the suitability of Cu@AC as adsorbent. Exactly, the observed increase in the proportion of dye elimination can be attributed to the greater availability of sorption surface and an increased capacity of the adsorption sites. As the dosage of the adsorbent increases, more active sites become accessible for adsorption, leading to a higher capacity for removing dyes from their solutions. This relationship leads to an overall increase in the efficiency of dye removal as already reported in the literatures by Alencar *et al*. (2012) and Tural *et al*. (2017).

Similar findings were observed regarding the adsorbent dosage's impact on dye removal. However, it is essential to highlight that for specific adsorbents, using high dosages caused agglomeration in the solution, which hindered further evolution of the percentage of dye removal beyond a certain equilibrium point. In such cases, excessively high dosages might not lead to increased efficiency in dye removal due to the adverse effects of agglomeration *(Lamari et al.,* 2022).

3.2.3. Effect of initial dye concentrations

The effect of initial dye concentration (from 25 to 65 mg/L) on the adsorption of MB and MO onto the Cu@AC was studied. The percentage of adsorption decreased as the initial concentration of MB increased, a trend consistent with the observations presented in Fig. 9. Indeed, the adsorption process is highly influenced by the initial concentration of dyes. At lower concentrations, the ratio of the initial number of dye molecules to the available surface area is low, leading to a situation where the fractional adsorption becomes independent of the initial concentration. In contrast, at higher dye concentrations, the available adsorption sites become limited, resulting in a higher dependence of the percentage removal of dyes on the initial concentration. In summary, the adsorption behavior varies significantly with the initial concentration of dyes, affecting the overall efficiency of the process.

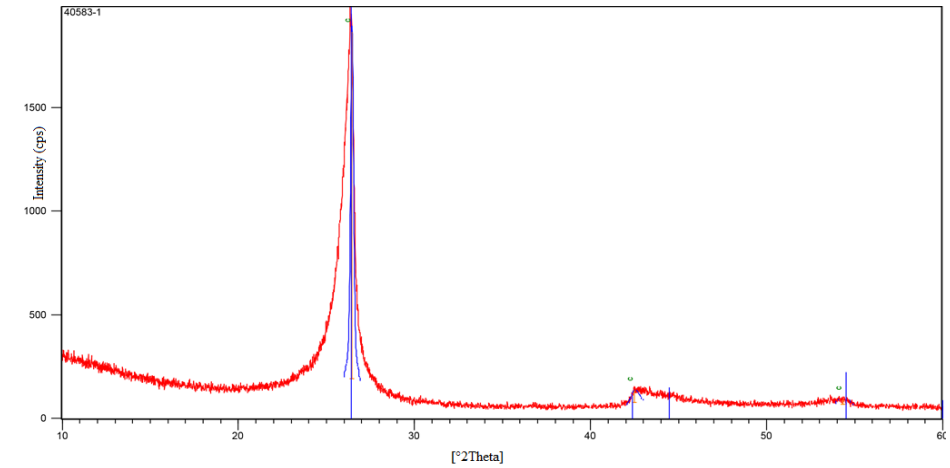

(a)

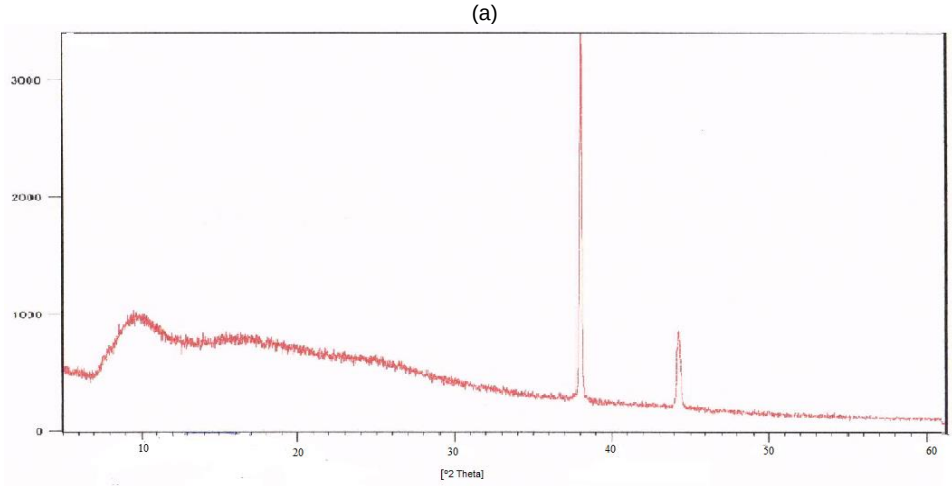

(b)

Fig. 6. XRD diffraction patterns of (a) AC, (b) Cu@AC.

The low dosage of Cu@AC (0.5 g) was insufficient to capture all the dye molecules, especially as the initial concentrations were raised, resulting in an abundance of dye molecules in the solution. Similar findings have been documented in prior studies involving various adsorbents and adsorbate combinations (Rápó and Tonk, 2021). On the other hand, in situations where there is an excess of adsorbate molecules, the availability of active sites for dye adsorption can become limited. To overcome this challenge and achieve cost-effective removal, two practical approaches can be employed: Using solutions with low initial dye concentration: By starting with a low concentration of dyes in the solution, the competition for adsorption sites is reduced, allowing for more effective and efficient removal of the dyes.

Employing high adsorbent dosage: Increasing the amount of adsorbent used in the process provides a larger number of active sites for adsorption, compensating for the excess of adsorbate molecules and improving the overall removal efficiency. Both of these approaches align with environmental requirements as they offer effective dye removal without using the highest adsorption capacity of the available active sites. Their application requires more practices in treating dye-contaminated wastewater.

3.2.4. Effect of contact time

Contact time is a critical factor that influences the removal of dyes through adsorption. Fig. 10 A illustrates the time-dependent elimination pattern of dyes from an aqueous solution using Cu@AC as the adsorbent. It is evident that for both dyes, the elimination increases as the contact time is prolonged. Specifically, the percentage of dye elimination has reached its maximum value of 100% for MO and 95% for MB within a time frame of 90 minutes when the solution is agitated in a shaker. This demonstrates the efficiency of the adsorbent in removing the dyes from the solution over the specified duration.

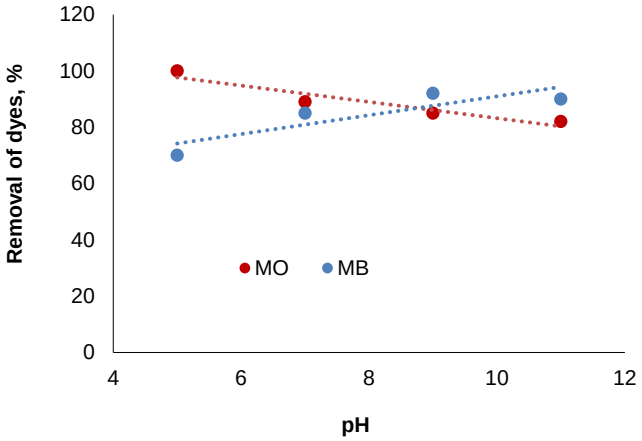

Fig. 7. Percent of dyes removal versus the pH of the solution.

As the contact time between the adsorbent and the dyes increases, the efficiency of dye removal also increases. Notably, the highest removal efficiency is observed within the initial minutes of contact, and the maximum removal efficiency for both dyes is achieved within about 90 minutes. The experimental results indicate that a significant portion of the adsorption occurs during the initial half-hour of contact, and the rate of dye removal increases at a slower pace after that. This suggests that the adsorption process is more rapid and efficient in the early stages of contact, and as time progresses, the rate of dye removal gradually slows down.

The experiments were conducted over a range of contact times, spanning from 10 to 90 min, to observe the variations in dye removal efficiency at different time intervals. The findings provide valuable insights into the kinetics of the adsorption process and help understand the optimal contact time required for achieving the highest removal efficiency. The adsorption of dyes involves multiple of step-

processes that contribute through the relatively longer contact time required for effective removal. The sequence of steps includes:

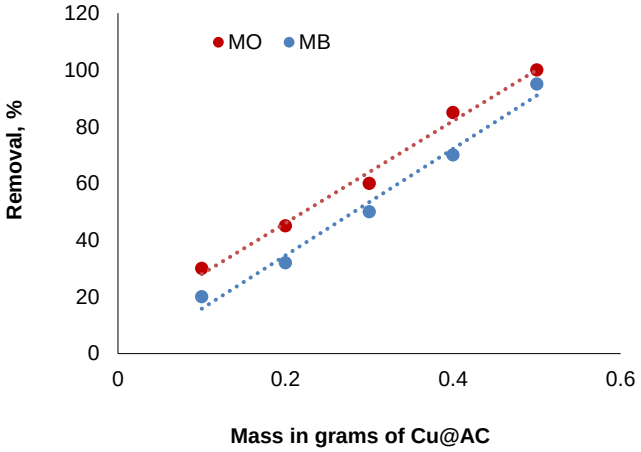

Fig. 8. Percent of dye removal versus adsorbent dose (pH = 5, C_o = 50 mg/L, t = 90 min, A.S. = 150 rpm, T = 298 K).

1. Boundary layer diffusion: Initially, the dye molecules reach the boundary layer surrounding the adsorbent particles. This is the region immediately adjacent to the adsorbent's surface where there might be concentration gradients.
2. Surface diffusion: Subsequently, the dye molecules need to diffuse into the adsorbent's surface. This step involves the migration of dye molecules from the boundary layer into the active sites or pores on the adsorbent's surface.
3. Pore diffusion: Finally, the dye molecules must diffuse further into the porous structure of the adsorbent to reach its interior. This process enables the dye molecules to access deeper layers of the adsorbent and maximize the adsorption capacity.

The combination of these diffusion steps results in a longer contact time requirement for achieving the highest removal efficiency. It is crucial to consider these aspects when designing and optimizing the adsorption process for efficient dye removal. As shown in Fig. 10 A, with an increase in contact time from 10-90 min, the dyes removal efficiency rises from 40 % to 100 % for MO and 25% to 95% for MB. Ammar and Abbas (2016) in their experiments conducted for removal of Fluoroquinolones antibiotics by AC found that increased contact time led to increased removal of Fluoroquinolones. After investigating different contact durations, they determined that the equilibrium point, where the removal efficiency stabilizes, was reached at 90 minutes. This implies that 90 minutes of contact time was identified as the optimal duration for achieving the highest efficiency in removing Fluoroquinolones antibiotics using AC as the adsorbent (Abbas, Ahmed, and Darweesh, 2016).

Based on the results of the experiment investigating the effect of contact time of Cu@AC (Copper-loaded Activated Carbon) as absorbent, it was observed that the efficiency of Cu@AC in removing dyes is higher than pristine AC (Fig.10 b). The higher removal efficiency of Cu@AC suggests that the incorporation of copper onto the activated carbon surface enhances its adsorption capabilities for dyes. This improvement is likely due to creation of additional adsorption sites and interactions of copper with adsorbants, leading to a more effective removal of dyes from the solution compared to using pristine AC.

3.2.5. Effect of temperature

Temperature plays a crucial role to consider when designing adsorption systems for various applications, as it can significantly impact the efficiency and capacity of the adsorbent. This effect was investigated at (298–333 K). Fig. 11 shows the adsorption capacity of Cu@AC increases by temperature from 298 to 333 K. Certain effects of temperature on the adsorption process includes:
1. Rate of diffusion: Raising the temperature causes a reduction in solution viscosity, which, consequently, enhances the rate of diffusion of adsorbate molecules across both the internal pores of the adsorbent particles and the external boundary layer. This heightened diffusion rate facilitates a swifter adsorption process, enabling adsorbate molecules to adhere to the adsorbent's surface and infiltrate its porous structure more rapidly.
2. Equilibrium capacity: Temperature changes can influence the equilibrium capacity of the adsorbent for a specific adsorbate. In many cases, an increase in temperature results in a higher equilibrium capacity, meaning that the adsorbent can adsorb more of the adsorbate at higher temperatures.

Both of these effects play crucial roles in optimizing the adsorption process and understanding the temperature dependence of adsorption behavior.

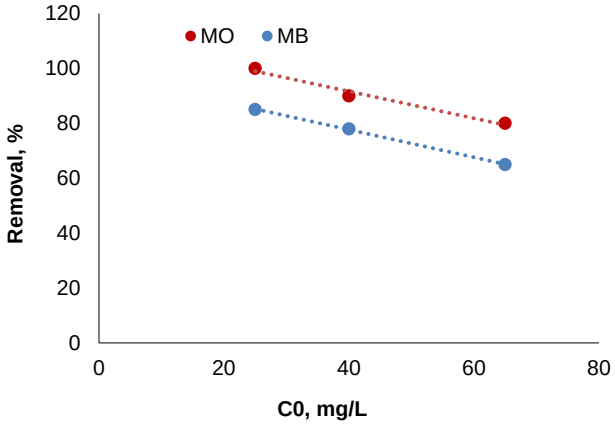

Fig. 9. Percent of dye removal by Cu@AC (pH = 5; stirring speed: 150 rpm; adsorbent dosage: 0.5 g; T = 298 K; contact time 90 min) versus initial concentration of MO and MB.

In the Fig. 11, the temperature was set at 298, 313, and 333 K for studying a solution (25 mL) of dye (25 mg/L) mixed with 0.5 g of Cu@AC by shaking at 150 rpm for 90 min. Fig. 11 shows that the dye removal increased as the temperature rose. It is anticipated that increase of adsorption by temperature would be due to a reduction in viscosity of the dye solution. This effect enhances the mobility of the absorbent particles, facilitating the adsorption process. The experimental findings confirmed that the removal of dyes was more effective at higher temperatures. This observation suggests that the adsorption processes involved are endothermic, meaning that they are favored and enhanced by higher temperatures. The higher mobility of the dye molecules at elevated temperatures cause to found an enhanced diffusion toward the adsorbent surface and to establish stronger interactions with the active sites of Cu@AC, leading to an improved adsorption efficiency (Munyegaju *et al.*, 2022).

Overall, the increased mobility of the dye molecules and their enhanced interaction with the active sites of Cu@AC at higher temperatures contribute to the improved adsorption efficiency, making it a favorable choice for dye removal applications within the appropriate temperature range.

3.2.6. Effect of different eluents and reusability

Desorption studies serve as a critical endeavor with two primary goals: managing sludge and assessing the potential for reusing the adsorbent after the sorption process. By understanding desorption characteristics, researchers can optimize the adsorption-desorption process for efficient pollutant removal while ensuring the economic and environmental viability of the treatment approach. Reusable adsorbents play a crucial role in practical applications, making them highly valuable in various environmental remediation processes and wastewater treatment technologies.

Adsorption of MB and MO on activated carbon doped with copper II is a reversible process. Therefore, regeneration or reactivation of Cu@AC is possible for reuse. Dyes removal from Cu@AC was studied using different types of solvents including acid, base, alcohols, and organic solvents.

Table 3 shows the recovery percentage of methyl orange and methylene blue dyes absorbent with different eluents. From Table 3, it can be concluded that 2.0 ml of NaOH solution (0.1 M) is the most effective detergent to remove MO from the surface of Cu@AC. The findings showed that by using one-step washing with NaOH solution in less than 5 minutes, the recovery efficiency of methyl orange dye absorbent is more than 99%

MO dye can be desorbed from Cu@AC by changing the pH of the washing-solution to the alkaline range. The adsorption and desorption study for dyes were also done with its own conditions and the results of the study are given in the Table 3. However, the removal of MB dye is performed by an HCl (0.1 M) solution with a high efficiency.

Under acidic conditions, the quantity of positively charged sites on the adsorbent rises. This increase promotes the desorption efficiency of MB dye because of the electrostatic repulsion occurring between the positively charged sites on Cu@AC and the MB cations.

Consequently, desorbing agents capable of generating more cations in the solution, particularly H^+ ions, are preferred eluents for desorbing cationic dyes. Another contributing factor could be the abundance of H+ ions in the acidic solution, leading to their exchange with the MB ions adsorbed on Cu@AC (Zein *et al.,* 2023).

The adsorbents can be recycled through multiple sorption/desorption cycles using the desorption process (Table 4). This significantly decreases the overall cost of the treatment procedure, minimizes the need for a constant supply of new adsorbents, and mitigates the challenges associated with disposing of spent adsorbents. Cu@AC was rinsed using deionized water and subsequently employed in two consecutive removal processes, exhibiting a removal efficiency exceeding 90% in each instance. With more removal cycles, the removal efficiency of the recycled adsorbent decreases. The observed phenomenon can be attributed to the oxidation, loss, and/or dissolution of specific portions of the adsorbent during the successive washing steps (Daneshvar *et al.,* 2017).

Table 3. The effect reagents on adsorbent recycling efficiency.

Eluents	HCl 0.1M	Acetic acid	EtOH	NaOH 0.1M
Adsorbent recycling efficiency of MO dye, %	20	75	85	100
Adsorbent recycling efficiency of MB dye, %	96	85	72	25

Table 4. The effect of cycles of regeneration on adsorption performance.

Adsorbent reuse	Cycle 1	Cycle 2	Cycle 3	Cycle 4
Efficiency of MO removal, %	100	91	57	20
Efficiency of MB removal, %	95	82	55	15

4. Conclusions

Copper-doped activated carbon with a high specific surface area (611 m^2/g) was produced by the chemical activation of natural bitumen at high temperature using H_3PO_4 as the activating agent. Natural bitumen is an ecologically friendly and economically efficient source material for producing activated carbon. Wastewater contaminated with dyes poses a grave threat to human health and reaching the goal of a sustainable environment. An effective adsorbent, Cu@AC, demonstrates efficient removal of representative dyes, including anionic MO and cationic MB, from contaminated water. Compared to the ordinary AC, the highest adsorption capacity of Cu@AC for adsorptive removal of the dyes from wastewater is significantly greater. The effects of main variables on efficacy of dye adsorption by Cu@AC were explored, indicating that removal of the dyes is maxima with initial dye concentration of 25 mg/L, pH of 9 for MB and pH of 5 for MO, and contact time of 90 min when using 0.5 g/L of Cu@AC as adsorbent. The maximum adsorption capacity was measured to be as high as 707 mg/g. The adsorption of MO or MB on Cu@AC at different temperatures shows that it is an endothermic process. We anticipate Cu@AC will receive more attention from researchers since it can play a catalytic role in many organic reactions and can be regarded as a promising adsorbent for removal of other organic pollutants from aqueous streams.

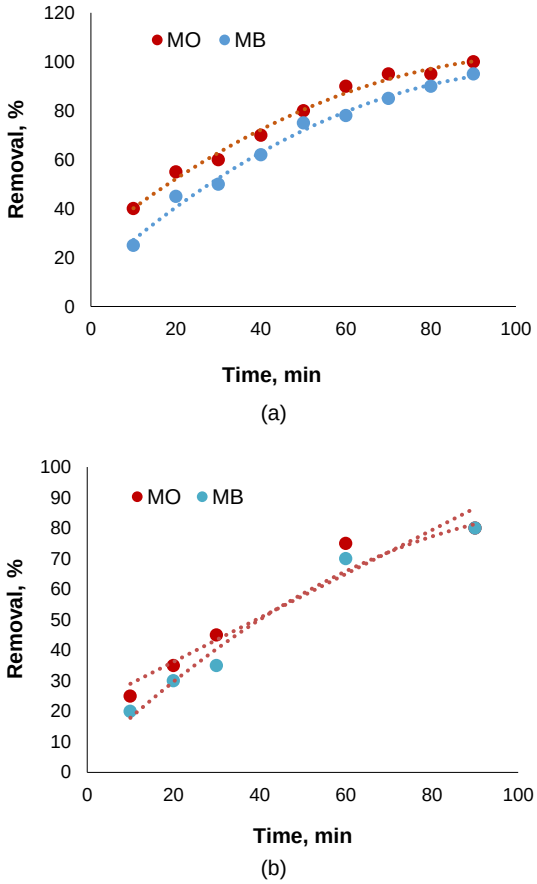

Fig. 10. (a) The effect of contact time on dyes removal efficiency by using Cu@AC, and (b) AC.

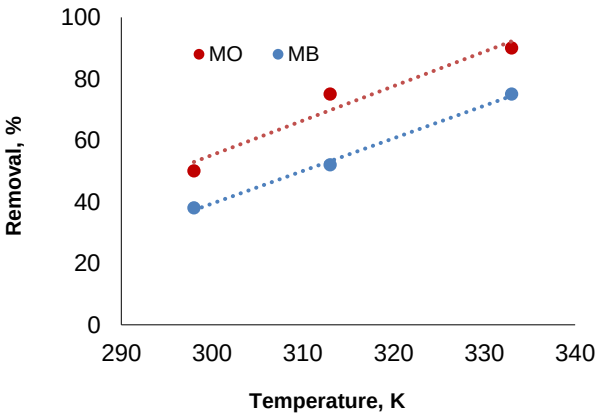

Fig. 11. The effect of temperature on dyes removal efficiency.

Author Contributions

Zahra Fadaei: Conceptualization, methodology, writing - original draft & editing, data curation, investigation, formal analysis, validation. Kurosh Rad-Moghadam: Supervision and designing of project. Parvaneh Pakravan: Writing assistance, technical editing, language editing and proof reading.

Conflict of Interest

The authors declare no competing interests and non-financial competing interests.

Acknowledgement

The authors are grateful to research council of University of Guilan (Rasht, Iran) for partial supports of this work and want to thank Kermanshah Academic Center for Education, Culture and Research

(ACECR) (Kermanshah, Iran) to supply the laboratory additional equipment and materials.

Data Availability Statement

The datasets used and/or analyzed during the current study are available from the corresponding author on reasonable request.

References

Abbas A.S., Ahmed M.J., and Darweesh T.M. (2016) 'Adsorption of fluoroquinolones antibiotics on activated carbon by K_2CO_3 with microwave assisted activation', *Iraqi Journal of Chemical and Petroleum Engineering,* 17(2)**,** pp. 15-23. doi: https://doi.org/10.31699/IJCPE.2016.2.3

Abbass, R. *et al.* (2022) 'Using the aluminum decorated graphitic-C3N4 quantum dote (QD) as a sensor, sorbent, and photocatalyst for artificial photosynthesis; a DFT study', *Journal of Molecular Graphics and Modelling,* 117, 108302. doi: https://doi.org/10.1016/j.jmgm.2022.108302

Abdedayem A., Guiza M., and Ouederni A. (2015) 'Copper supported on porous activated carbon obtained by wetness impregnation: Effect of preparation conditions on the ozonation catalyst's characteristics', *Comptes Rendus Chimie,* 18(1)**,** pp. 100-109. doi: https://doi.org/10.1016/j.crci.2014.07.011

Alencar, W. S. *et al.* (2012) 'Application of Mangifera indica (mango) seeds as a biosorbent for removal of Victazol Orange 3R dye from aqueous solution and study of the biosorption mechanism', *Chemical Engineering Journal,* 209, pp. 577-588. doi: http://doi.org/10.1016/j.cej.2012.08.053

Ali, R. *et al.* (2020) 'BET, FTIR, and RAMAN characterizations of activated carbon from waste oil fly ash', *Turkish Journal of Chemistry,* 44(2)**,** pp. 279-295. doi: http://doi:10.3906/kim-1909-20

Alsukaibi, A. K. D. (2022) 'Various approaches for the detoxification of toxic dyes in wastewater', *Processes*, 10(10), 1968. doi: ARWW-2309-1307 (R2)-5-21 new.docx

Annadurai G., Juang R.S., and Lee D.J. (2002) 'Use of cellulose-based wastes for adsorption of dyes from aqueous solutions', *J Hazard Mater,* 92(3)**,** pp. 263-74. doi: https://doi.org/10.1016/S0304-3894(02)00017-1

Anupam, K. *et al.* (2023) 'A state-of-the-art review of natural bitumen in pavement: Underlining challenges and the way forward', *Journal of Cleaner Production,* 382, 134957. doi: https://doi.org/10.1016/j.jclepro.2022.134957

Ayar A., Gezici O. and Küçükosmanoğlu M. (2007) 'Adsorptive removal of Methylene blue and Methyl orange from aqueous media by carboxylated diaminoethane sporopollenin: On the usability of an aminocarboxilic acid functionality-bearing solid-stationary phase in column techniques', *Journal of Hazardous Materials,* 146(1)**,** pp. 186-193. doi: https://doi.org/10.1016/j.jhazmat.2006.12.009

Azam, K. *et al.* (2022) 'A review on activated carbon modifications for the treatment of wastewater containing anionic dyes', *Chemosphere,* 306, 135566. doi: https://doi.org/10.1016/j.chemosphere.2022.135566

B. Cevallos Toledo, R. *et al.* (2020) 'Reactivation process of activated carbons: Effect on the mechanical and adsorptive properties', *Molecules,* 25(7)**,** p. 1681. doi: http://doi.org/10.3390/molecules25071681

Bahramifar N., Tavasolli M., and Younesi H. (2015) 'Removal of eosin Y and eosin B dyes from polluted water through biosorption using Saccharomyces cerevisiae: Isotherm, kinetic and thermodynamic studies', *Journal of Applied Research in Water and Wastewater,* 2(1)**,** pp. 108-114. Available at: https://arww.razi.ac.ir/article_229_26401140ba4fd0c72b1fc988058f7b4d.pdf (Accessed date: 10 June 2023).

Brishti, R. S. *et al.* (2023) 'Adsorption of iron(III) from aqueous solution onto activated carbon of a natural source: Bombax ceiba fruit shell', *Results in Chemistry,* 5, 100727. doi: https://doi.org/10.1016/j.rechem.2022.100727

Cui, Y. *et al.* (2020) 'In situ preparation of copper-loaded carbon-based catalyst with chelate resin and its application on persulfate activation for X-3B degradation', *Catalysts,* 10(11)**,** p. 1333. doi: https://doi.org/10.3390/catal10111333

Daneshvar, E. *et al.* (2017) 'Desorption of methylene blue dye from brown macroalga: Effects of operating parameters, isotherm study and kinetic modeling', *Journal of Cleaner Production,* 152, pp. 443-453. doi: https://doi.org/10.1016/j.jclepro.2017.03.119

Danmaliki, G. I., and Saleh, T. A. (2017) 'Effects of bimetallic Ce/Fe nanoparticles on the desulfurization of thiophenes using activated carbon', *Chemical engineering journal,* 307, pp. 914-927. doi: https://doi.org/10.1016/j.cej.2016.08.143

De Gisi, S. *et al.* (2016) 'Characteristics and adsorption capacities of low-cost sorbents for wastewater treatment: A review', *Sustainable Materials and Technologies,* 9, pp. 10-40. doi: https://doi.org/10.1016/j.susmat.2016.06.002

Elango, M. *et al.* (2017) 'Synthesis, characterization, and antibacterial activity of polyindole/Ag–Cuo nanocomposites by reflux condensation method', *Polymer-Plastics Technology and Engineering***,** 57(14), pp. 1-12. doi: https://doi.org/10.1080/03602559.2017.1410832

Ghasemian Lemraski E., Sharafinia S. and Alimohammadi M. (2017) 'New activated carbon from persian mesquite grain as an excellent adsorbent', *Physical Chemistry Research,* 5(1)**,** pp. 81-98. doi: https://doi.org/10.22036/pcr.2017.38495

Ghorbani, F. and Kamari, S. (2016) 'Application of response surface methodology for optimization of methyl orange adsorption by Fe-grafting sugar beet bagasse', *Adsorption Science & Technology,* 35(3-4)**,** pp. 317-338. doi: https://doi.org/10.1177/0263617416675625

Haque E., Jun J.W., and Jhung S.H. (2011) 'Adsorptive removal of methyl orange and methylene blue from aqueous solution with a metal-organic framework material, iron terephthalate (MOF-235)', *Journal of Hazardous Materials,* 185(1)**,** pp. 507-511. doi: https://doi.org/10.1016/j.jhazmat.2010.09.035

Hosseini, S. *et al.* (2015) 'Adsorption of carbon dioxide using activated carbon impregnated with Cu promoted by zinc', *Journal of the Taiwan Institute of Chemical Engineers,* 52, pp. 109-117. doi: https://doi.org/10.1016/j.jtice.2015.02.015

Hung, N. V. *et al.* (2022) 'Highly effective adsorption of organic dyes from aqueous solutions on longan seed-derived activated carbon', *Environmental Engineering Research,* 28(3)**,** 220116. doi: https://doi.org/10.4491/eer.2022.116

Jiang, S. *et al.* (2018a) 'Cu-MFI zeolite supported on paper-like sintered stainless fiber for catalytic wet peroxide oxidation of phenol in a batch reactor', *Separation and Purification Technology,* 190 (pp. 243-251. doi: https://doi.org/10.1016/j.seppur.2017.09.001

Jiang S., Zhang H., and Yan Y. (2018b) 'Synthesis of copper-loaded activated carbon for enhancing the photocatalytic removal of methylene blue', *Journal of Molecular Liquids,* 272, pp. 353-360. doi: https://doi.org/10.1016/j.molliq.2018.09.087

Kamdod, A. S., and Kumar, M. V. P. (2022) 'Adsorption of methylene blue, methyl orange, and crystal violet on microporous coconut shell activated carbon and Its composite with chitosan: Isotherms and kinetics', *Journal of Polymers and the Environment,* 30(12)**,** pp. 5274-5289. doi: https://doi.org/10.5004/dwt.2022.28270

Khodaie, M. *et al.* (2013) 'Removal of methylene blue from wastewater by adsorption onto ZnCl2 activated corn husk carbon equilibrium studies', *Journal of Chemistry,* 2013, 383985. doi: https://doi.org/10.1155/2013/383985

Lamari R., Benotmane B., and Mostefa F. (2022) 'Removal of methyl orange from aqueous solution using zeolitic imidazolate framework-11: Adsorption isotherms, kinetics and error analysis', *Iranian Journal of Chemistry and Chemical Engineering,* 41(6)**,** pp. 1985-1999. doi: https://doi.org/10.30492/IJCCE.2021.131068.4236

Masoudian S., Rasoulifard M.H. and Pakravan P. (2015) 'Degradation of acid red 14 in contaminated water by Ag-SiO_2 nanocomposite', *Indian Journal of Chemistry A (IJC-A),* 54 A(6)**,** pp. 757-761. https://nopr.niscpr.res.in/bitstream/123456789/31678/2/IJCA%2054A(6)%20757-761.pdf (Accessed date: 24 June 2023).

Mishra, D. *et al.* (2022) 'Bitumen and asphaltene derived nanoporous carbon and nickel oxide/carbon composites for supercapacitor electrodes', *Scientific Reports,* 12(1)**,** pp. 4095. doi: https://doi.org/10.1038/s41598-022-08159-3

Munyegaju, J. *et al.* (2022) 'Textile effluent treatment using Avocado seeds based activated carbon', *Journal of Applied Research in*

Water and Wastewater, 9(1), pp. 83-90. doi: https://doi.org/10.22126/arww.2022.8008.1258

Ngueabouo, A. M. S. *et al.* (2022) 'Strategy for optimizing the synthesis and characterization of activated carbons obtained by chemical activation of coffee husk', *Materials Advances,* 3(22), pp. 8361-8374. doi: https://doi.org/10.1039/D2MA00591C

Pakravan, P. (2017) 'The possibility of selective Adsorption and sensing of the noble gaseous species by the C20 fullerene, the graphene sheets, and the N_4B_4 cluster', *Journal of Physical & Theoretical Chemistry,* 14(1), pp. 15-24. https://jptc.srbiau.ac.ir/article_10951.html (Accessed date: 11 July 2023).

Pakravan, P. (2018) 'Spontaneous adsorption, and selective sensing of CO, and CO_2 greenhouse gaseous species by the more stable forms of N_4B_4 clusters', *Physical Chemistry Research,* 6(2), pp. 377-385. doi: https://doi.org/10.22036/pcr.2018.111823.1444

Quine, C. M. *et al.* (2022) 'Hydrogen adsorption and isotope mixing on copper-functionalized activated carbons', *The Journal of Physical Chemistry C,* 126(39), pp. 16579-16586. doi: https://doi.org/10.1021/acs.jpcc.2c02960

Rápó, E. and Tonk, S. (2021) 'Factors affecting synthetic dye adsorption; desorption studies: A review of results from thelast five years (2017-2021)', *Molecules,* 26(17), 5419. doi: https://doi.org/10.3390/molecules26175419

Rocher, V. *et al.* (2008) 'Removal of organic dyes by magnetic alginate beads', *Water Research,* 42(4), pp. 1290-1298. doi: https://doi.org/10.1016/j.watres.2007.09.024

Saka, C. (2012) 'BET, TG–DTG, FT-IR, SEM, iodine number analysis and preparation of activated carbon from acorn shell by chemical activation with ZnCl2', *Journal of Analytical and Applied Pyrolysis,* 95, pp. 21-24. doi: https://doi.org/10.1016/j.jaap.2011.12.020

Shafeii Darabi S.F., Bahramifar N. and Khalilzadeh M.A. (2018) 'Equilibrium, thermodynamic and kinetics studies on adsorption of eosin Y and red X-GRL from aqueous solution by treated rice husk', *Journal of Applied Research in Water and Wastewater,* 5(1), pp. 392-398. doi: https://doi.org/10.22126/arww.2018.866

Shahrezaei, F. *et al.* (2018) 'Photoinduced pyrene degradation in contaminated soils by polyaniline coated photocatalysts', *Indian Journal of Chemistry A (IJCA),* 57(5), pp. 610-618. https://nopr.niscpr.res.in/bitstream/123456789/44396/1/IJCA%2057A%285%29%20610-618.pdf (Accessed date: 9 August 2023).

Sharma, S. *et al.* (2021) 'Biomass-derived activated carbon-supported copper catalyst: An efficient heterogeneous magnetic catalyst for base-free Chan–Lam coupling and oxidations', *American Chemical Society Omega,* 6(30), pp. 19529-19545. doi: https://doi.org/10.1021/acsomega.1c01830

Shu, J. *et al.* (2017) 'Copper loaded on activated carbon as an efficient adsorbent for removal of methylene blue', *Royal Society of Chemistry advances,* 7(24), pp. 14395-14405. doi: https://doi.org/10.1039/C7RA00287D

Trung, N. D. *et al.* (2022) 'Fabrication of metal loaded activated carbon by carbothermal functionalization of agriculture waste via ultrasonic-assisted technique for dye adsorption', *Vietnam Journal of Chemistry,* 60(4), pp. 546-551. doi: https://doi.org/10.1002/vjch.202200032

Tural, B. *et al.* (2017) 'Preparation and characterization of a novel magnetic biosorbent functionalized with biomass of Bacillus Subtilis: Kinetic and isotherm studies of biosorption processes in the removal of Methylene Blue', *Journal of Environmental Chemical Engineering,* 5(5), pp. 4795-4802. doi: http://dx.doi.org/10.1016/j.jece.2017.09.019

Ullah, A. *et al.* (2022) 'Removal of methylene blue from aqueous solution using black tea wastes: Used as efficient adsorbent', *Adsorption Science & Technology,* 2022, 5713077. doi: https://doi.org/10.1155/2022/5713077

Vunain E., Kenneth D., and Biswick T. (2017) 'Synthesis and characterization of low-cost activated carbon prepared from Malawian baobab fruit shells by H3PO4 activation for removal of Cu(II) ions: equilibrium and kinetics studies', *Applied Water Science,* 7(8), pp. 4301-4319. doi: https://doi.org/10.1007/s13201-017-0573-x

Wang J., Ma J., and Sun Y. (2022) 'Adsorption of methylene blue by coal-based activated carbon in high-salt wastewater', *Water,* 14(21), 3576. doi: https://doi.org/10.3390/

Xue, H. *et al.* (2022) 'Adsorption of methylene blue from aqueous solution on activated carbons and composite prepared from an agricultural waste biomass: A comparative study by experimental and advanced modeling analysis', *Chemical Engineering Journal,* 430, 132801. doi: https://doi.org/10.1016/j.cej.2021.132801

Yu, L. and Luo, Y.-M. (2014) 'The adsorption mechanism of anionic and cationic dyes by Jerusalem artichoke stalk-based mesoporous activated carbon', *Journal of Environmental Chemical Engineering,* 2(1), pp. 220-229. doi: https://doi.org/10.1016/j.jece.2013.12.016

Zein, R. *et al.* (2023) 'Enhancing sorption capacity of methylene blue dye using solid waste of lemongrass biosorbent by modification method', *Arabian Journal of Chemistry,* 16(2), 104480. doi: https://doi.org/10.1016/j.arabjc.2022.104480

Zhao, D. *et al.* (2020) 'Carbon nanotube-supported Cu-based catalysts for oxidative carbonylation of methanol to methyl carbonate: effect of nanotube pore size', *Catalysis Science & Technology,* 10(8), pp. 2615-2626. doi: https://doi.org/10.1039/C9CY02407G